ELSEVIER

Biochimica et Biophysica Acta 1457 (2000) 157–165

BIOCHIMICA ET BIOPHYSICA ACTA
BBA

www.elsevier.com/locate/bba

pH-Dependent characteristics of Y_Z radical in Ca^{2+}-depleted Photosystem II studied by CW-EPR and pulsed ENDOR

Hiroyuki Mino [a,*], Asako Kawamori [b], Taka-aki Ono [a]

[a] *Laboratory for Photo-Biology, RIKEN Photodynamics Research Center, The Institute of Physical and Chemical Research, 19-1399 Koeji, Nagamachi, Aoba, Sendai 980-0868, Japan*

[b] *Faculty of Science, Kwansei Gakuin University, Nishinomiya 662-8501, Japan*

Received 28 June 1999; received in revised form 5 January 2000; accepted 24 January 2000

Abstract

The Y_Z-tyrosine radical was trapped by freezing immediately after illumination in Ca^{2+}-depleted Photosystem II (PS II) membranes and the pH-dependent characteristics of the radical were investigated using CW-EPR and pulsed ENDOR. The spectrum of the $Y_Z^{\bullet}$ radical trapped in the $Y_Z^{\bullet}S_1$ state at pH 5.5 was cation-like as reported in Mn-depleted PS II (H. Mino et al., Spectrochim. Acta A 53 (1997) 1465–1483). By illuminating the PS II-retaining S_2 state, the $Y_Z^{\bullet}$ radical and a broad doublet signal formed in the $g \approx 2$ region were trapped concomitantly. The spectrum of the trapped $Y_Z^{\bullet}$ radical in the $Y_Z^{\bullet}S_2$ state was cation-like at pH 5.5 but the pulsed ENDOR measurements reveals the involvement of the neutral $Y_Z^{\bullet}$ radical in the doublet signal. At pH 7.0, the resulting $Y_Z^{\bullet}$ signal was the mixture of the cation-like and neutral radical spectra, and considerably different from the neutral radical found in Mn-depleted PS II. pH-Dependent changes in the properties of the $Y_Z^{\bullet}$ radical are discussed in relation to the redox events occurring in Ca^{2+}-depleted PS II.

Keywords: Photosystem II; Tyrosine Z; ENDOR; Ca^{2+} depletion; Doublet signal; pH dependence

1. Introduction

Photosynthetic water oxidation is carried out by an oxygen evolving center (OEC) composed of a tetra-nuclear Mn-cluster located at the lumenal side of Photosystem (PS) II protein complexes. Oxidized equivalents generated in the PS II reaction center by the successive absorption of four photons accumulate on the Mn-cluster and are used for water oxidation. A molecular oxygen is produced by reactions with five kinetically characterized intermediate states labeled S_i ($i = 0$–4), where S_1 is thermally stable in the dark. By absorbing each photon, the S_1 state advances stepwise to reach the highest oxidation state, S_4, that decays spontaneously to the S_0 state with concurrent release of a molecular oxygen (reviewed in [1–3]). S-state transitions are accompanied by cyclic changes in the oxidation state of the Mn-cluster [4,5], although the valences of manganese ions in the respective S-states remain a matter of debate.

The oxidation of the Mn-cluster by an oxidized reaction center of PS II ($P680^+$) is mediated by a

Abbreviations: MES, 2-morpholinoethanesulfonic acid; MOPS, 4-morpholinopropanesulfonic acid; DCMU, 3-(3,4-dichlorophenyl)-1,1-dimethylurea; ENDOR, electron nuclear double resonance; ESE, electron spin echo; ESEEM, electron spin echo envelope modulation

* Corresponding author. Fax: +81-22-228-2045;
E-mail: mino@postman.riken.go.jp

0005-2728/00/$ – see front matter
PII: S0005-2728(00)00074-8

redox-active tyrosine residue (Tyr 161) of the D1 protein regarded as Y_Z (reviewed in [1–3]). Y_Z is oxidized to a radical by $P680^+$, and the $Y_Z^\bullet$ radical is quickly reduced by delivery of an electron from the Mn-cluster. The radical is, however, rather stable in the absence of the Mn-cluster and reveals a typical EPR signal called Signal II_f (reviewed in [1,3]). The other redox-active tyrosine residue (Y_D) in the D_2 protein (Tyr 161) is present in PS II, and it functions as an auxiliary redox component. The oxidized form of Y_D is very stable in the dark, and shows an EPR signal called Signal II_s. Both EPR signals had shown very similar hyperfine splitting with an intensity ratio of about 1:3:3:1 which arises from coupling with one of the β-methylene protons and two equivalent $C_{(3),(5)}$-ring protons except for a slight difference attributable to the difference in the dihedral angle of the β-methylene proton [6,7]. ESEEM results imply that a neutral tyrosine radical is responsible for Signal II_s [8]. On the basis of the similarity in the lineshape between the Signal II_f and Signal II_s, $Y_Z^\bullet$ has been considered to be a neutral radical also [6–9].

We reported that the EPR and pulsed-ENDOR spectra of $Y_Z^\bullet$ in Mn-depleted PS II membranes change in a pH-dependent manner [10]. Above pH 6.5, the spectrum of the $Y_Z^\bullet$ radical is quite similar to that of the $Y_D^\bullet$ radical that is assigned as neutral in consistent with previously reported results [6–8]. The spectrum is, however, distinct from the $Y_D^\bullet$ spectrum below pH 6.0, and can be reasonably simulated by assuming a cation-like distribution of spin density on a tyrosine molecule. These results are thought to indicate that the oxidized Y_Z exists as a neutral radical above pH 6.5 but as a cation-like radical below pH 6.0 in Mn-depleted PS II. The Y_Z tyrosine may function not only as a simple electron mediator between P680 and the Mn-cluster but also as part of the water oxidation machinery, in which the protonation and deprotonation of Y_Z directly contribute to the proton abstraction from water molecules. Therefore, it is important to define whether or not Y_Z is oxidized to a cation-like radical in the presence of the Mn-cluster.

In oxygen-evolving PS II, photogenerated $Y_Z^\bullet$ is detectable at room temperature only by time-resolved spectroscopy, which may not generate a sufficiently high quality of spectrum. The $Y_Z^\bullet$ radical, however, can be trapped by rapid freezing after illumination at about 253 K in Ca^{2+}-depleted PS II that preserves the Mn-cluster [11]. In this paper, we describe the effect of pH on EPR and pulsed ENDOR signals of the $Y_Z^\bullet$ radical trapped in Ca^{2+}-depleted PS II. The spectrum of the trapped radical changed in a manner that was pH-dependent and similar to that found in Mn-depleted PS II. The results indicated that the Y_Z is oxidized to a cation-like radical even in the presence of the Mn-cluster.

2. Materials and methods

Oxygen-evolving PS II membranes were prepared from spinach as described [12] with modifications [13]. For Ca^{2+}-depletion, the membranes were washed twice with a medium containing 400 mM sucrose, 20 mM NaCl and 0.1 mM MES/NaOH (pH 6.5), then suspended in the same medium. The membranes were then suspended in a medium containing 400 mM sucrose, 20 mM NaCl, 10 mM citric acid/NaOH (pH 3.0) at 0°C for 5 min, then 10% volume of a solution containing 400 mM sucrose, 20 mM NaCl and 500 mM MOPS/NaOH (pH 7.5) was added to adjust the final pH to about 6.5, as described [14]. The treated membranes were washed and resuspended in a buffer medium containing 400 mM sucrose, 20 mM NaCl and 20 mM MES/NaOH (pH 5.5–7.0). All manipulations proceeded in the dark or under a dim green light to maintain the OEC in the S_1 state unless otherwise noted. Aliquots of the Ca^{2+}-depleted membrane samples (0.5 mgChl/ml) were illuminated at 0°C for 1 min followed by dark-adaptation at 0°C for 30 min to prepare the OEC in the dark-stable S_2 state [15]. DCMU (50 μM, 10 mM dimethyl sulfoxide solution as stock) was added to the S_1 and S_2 states sample membranes to ensure a single turnover. For Mn-depletion, the membranes were incubated with 800 mM Tris (pH 8.0) under room light at 0°C for 30 min [16].

Membrane samples were collected by centrifugation at $35\,000 \times g$ for 20 min, transferred to Suprasil quartz tubes with a 4-mm inner diameter, purged by Ar gas and stored in liquid N_2 in sealed tubes. The final chlorophyll concentration was approximately 20 mgChl/ml. EPR samples were illuminated with a 500 W tungsten-halogen lamp through 8 cm path length of water for 15 s and 5 s at 253 K in the S_1

state Ca^{2+}-depleted and Mn-depleted PS II membranes, respectively. The $Y_Z^{\bullet}$ radical was trapped by immersing the sample into liquid N_2 immediately after illumination. After measuring the spectrum of the illuminated membranes, the samples were dark-adapted for 30 min at 0°C for complete decay of the $Y_Z^{\bullet}$ radical. The $Y_Z^{\bullet}$ spectrum was obtained by subtracting the dark-adapted spectrum from the illuminated spectrum. Alternatively, the sample membranes in the dark-stable S_2 state were illuminated for 60 s at 0°C to produce a $g \approx 2$ doublet signal followed by rapid freezing in liquid N_2. The characteristic β-methylene proton ENDOR signal of $Y_D^{\bullet}$ served as the internal standard to normalize the intensity of the pulsed ENDOR spectrum [10].

Electron spin echo experiments were performed on Bruker ESP-380 pulsed EPR spectrometer equipped with a cylindrical dielectric cavity (ER4117DHQ-H, Bruker) and a gas flow temperature control system (CF935, Oxford Instruments). Microwave (m.w.) pulses of 16 and 32 ns duration for $\pi/2$-π pulses were used for 2-pulse (primary) ESE sequence. Field-swept ESE spectra were measured by 2-pulse sequence with a time interval τ of 200 ns between the m.w. pulses. Pulsed ENDOR measurements used the sequence of m.w. and radiofrequency (rf) pulses introduced by Davies [17]. The durations of the m.w. pulses were 96, 48 and 96 ns. The separation between the first and the second m.w. pulses was 8 μs and that between the second and the third m.w. pulses was 200 ns. The 6-μs rf pulse was amplified using a 500 W amplifier (ENI 500A), and applied between the first and the second m.w. pulses. The external magnetic field was fixed at the peaks of the $Y_Z^{\bullet}$ and $Y_D^{\bullet}$ signals, or at the peak of the doublet signal on the high-field side.

CW-EPR spectra were measured by JEOL JES-FE1XG X-band EPR spectrometer. A finger-type Dewar was used for measurements at 77 K.

3. Results

Fig. 1 shows the X-band CW-EPR spectra (Fig. 1A) and pulsed ENDOR spectra (Fig. 1B) in Ca^{2+}-depleted (traces a, b and c) and Mn-depleted (trace d) PS II membranes at pH 7.0. Panel A shows that illumination followed by rapid freezing generated a spectrum composed of the $Y_D^{\bullet}$ and the trapped $Y_Z^{\bullet}$ radicals (trace a), and that the signal intensity was decreased by dark-adaptation at 0°C for 30 min (trace b) due to $Y_Z^{\bullet}$ dissipation. The lineshape of the $Y_Z^{\bullet}$ spectrum (trace c) obtained by subtracting the dark-adapted from the illuminated spectrum is less resolved than that of $Y_D^{\bullet}$. This is in contrast with the $Y_Z^{\bullet}$ spectrum found in Mn-depleted PS II membranes (trace d) that was quite similar to the $Y_D^{\bullet}$ spectrum (trace b). The $Y_D^{\bullet}$ spectrum was not visibly altered between Ca^{2+}-depleted and Mn-depleted membranes (data not shown).

Fig. 1B shows that the pulsed ENDOR spectrum of the $Y_D^{\bullet}$ radical (trace b) contains three peaks labeled A, B and C at 25, 28 and 31 MHz, corresponding to proton signals with hyperfine splittings of 20, 27, and 31 MHz, respectively. The peaks A/A′ have been assigned to $H_{(3)}$ and $H_{(5)}$ protons on the phenol ring of the tyrosyl radical [10,18–20]. Peaks B and C are ascribed to one of the β-methylene protons H_β with the perpendicular (peak B) and parallel (peak C) orientations, respectively, of the hyperfine tensor axis with respect to the static magnetic field $\boldsymbol{H_0}$ [10,18–20]. The spectrum of the sample membranes illuminated for trapping the $Y_Z^{\bullet}$ radical in Ca^{2+}-depleted membranes (trace a) differed considerably from that after dark-adaptation (trace b). Illumination minus dark-adapted (trace a minus trace b) spectrum (trace c) revealed several new peaks labeled D/D′, E/E′ and G at around 20, 22 and 32 MHz of ENDOR frequency, corresponding to proton signals with hyperfine splittings of 11, 15.5 and 34 MHz, respectively. The spectrum was almost completely devoid of peaks B and C, indicating little contribution of the $Y_D^{\bullet}$ radical to the difference spectrum. The ENDOR spectrum of $Y_Z^{\bullet}$ thus obtained (trace c) differed considerably from that in Mn-depleted membranes (trace d): peaks D/D′ and E/E′ were more intense but peak F became less pronounced. Peak F has been ascribed to protons $H_{(3)}$ and $H_{(5)}$ on the phenol ring of the tyrosyl radical [10,18–20]. Peak G found in both Ca^{2+}- and Mn-depleted membranes, which was less pronounced in the Ca^{2+}-depleted membranes, has been attributed to the β-methylene proton typical of a neutral tyrosyl radical [10,18–20]. The presence of smaller hyperfine splitting in the $Y_Z^{\bullet}$ spectrum trapped in Ca^{2+}-depleted than in Mn-depleted membranes is consistent

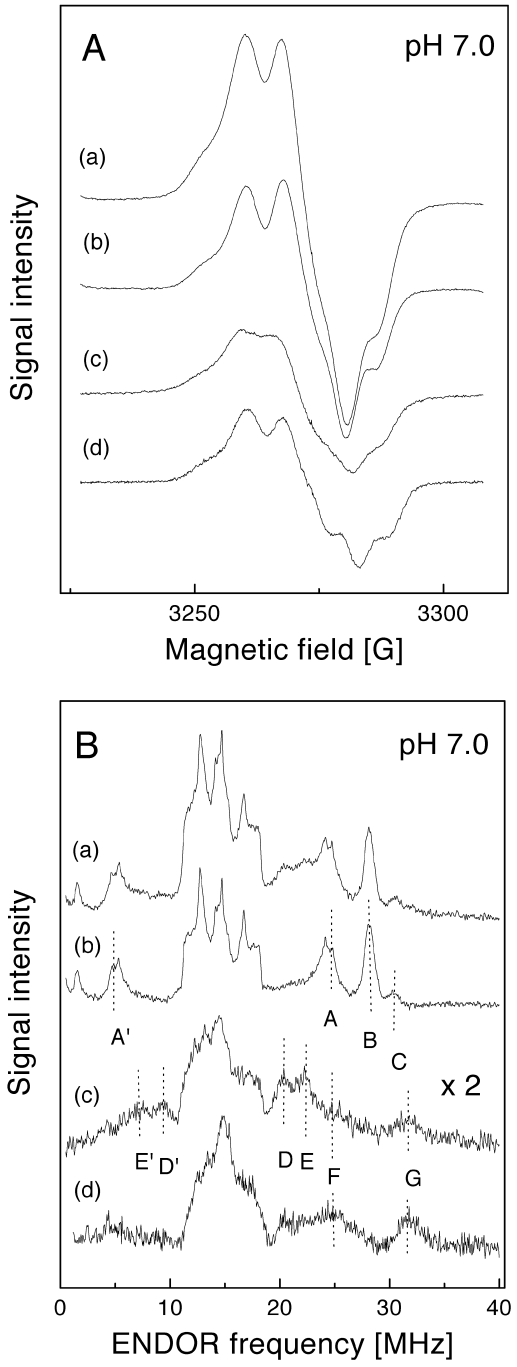

Fig. 1. CW-EPR (A) and pulsed ENDOR (B) spectra in Ca^{2+}-depleted PS II (a–c) and Mn-depleted PS II membranes (d) at pH 7.0. Ca^{2+}-depleted membranes were frozen rapidly after illumination for 15 s at 253 K (a) and dark-adapted for 30 min at 0°C (b). Mn-depleted membranes were illuminated for 5 s at 253 K, then dark-adapted for 30 min at 0°C. Illumination minus dark-adaptation difference spectra (c,d). DCMU (50 μM) was added to sample suspension before illuminating Ca^{2+}-depleted PS II membranes. CW-EPR conditions: microwave power, 0.05 mW; field modulation amplitude, 5 G at 100 kHz; temperature, 77 K. Davies pulsed ENDOR conditions: m.w. pulse lengths, $t^{\pi}_{mw} = 96$ ns, $t^{\pi/2}_{mw} = 48$ ns, $t^{\pi}_{mw} = 96$ ns and $t_{rf} = 6$ μs; temperature, 30 K.
←

with the less resolved CW spectrum of $Y^{\bullet}_Z$ in Ca^{2+}-depleted than Mn-depleted membranes shown in Fig. 1A.

Fig. 2 shows the X-band CW-EPR spectra (Fig. 2A) and pulsed ENDOR spectra (Fig. 2B) in Ca^{2+}-depleted PS II membranes (traces a–c) and Mn-depleted PS II membranes (trace d) at pH 5.5. Panel A shows that the CW-EPR spectrum of $Y^{\bullet}_Z$ radical was characteristic of broad EPR lineshapes in both Ca^{2+}-depleted (trace c) and Mn-depleted (trace d) membranes, in contrast to the $Y^{\bullet}_D$ radical spectra in which the lineshapes were well-resolved (trace b and [1,10,11,16]). As shown in panel B, the pulsed ENDOR spectra of the $Y^{\bullet}_Z$ radical had pronounced D/D′ and E/E′ peaks but no F and G peaks in both the membranes (traces c and d). The presence of distinct D/D′ and E/E′ peaks seems to be compatible with the unresolved line shape of the CW-EPR spectrum of the $Y^{\bullet}_Z$ radical in panel A. The D/D′ and E/E′ peaks correspond to proton signals with hyperfine splittings of 11 and 15.5 MHz that have been assigned to the NMR transition of the protons $H_{(3)}$ and $H_{(5)}$ on the ring carbons $C_{(3)}$ and $C_{(5)}$ of the tyrosine radical in Mn-depleted membranes [10].

The CW-EPR and pulsed ENDOR spectra of the trapped $Y^{\bullet}_Z$ radical in Ca^{2+}-depleted PS II membranes were quite different from those of a typical $Y^{\bullet}_Z$ spectrum measured at pH 7.0 in Mn-depleted PS II membranes. At a glance, one may presume that difference is attributable to the formation of the signals of Chl^+ and/or Car^+ radicals. Fig. 3 shows the X-band CW-EPR spectra (Fig. 3A) and pulsed ENDOR spectra (Fig. 3B) of Ca^{2+}-depleted PS II membranes at pH 5.5, in which we illuminated the membranes at 77 K in the presence of ferricyanide for the formation of both Chl^+ and Car^+ radicals [21–24]. Panel A shows that the illumination generated a spectrum composed of the $Y^{\bullet}_D$ and Chl^+/Car^+ signals (trace a), and the signal intensity was decreased by dark-adaptation at 0°C for 30 min (trace b). Subtraction of the dark-adapted from the illuminated spectrum gives a typical Chl^+/Car^+ signal at $g = 2.002$

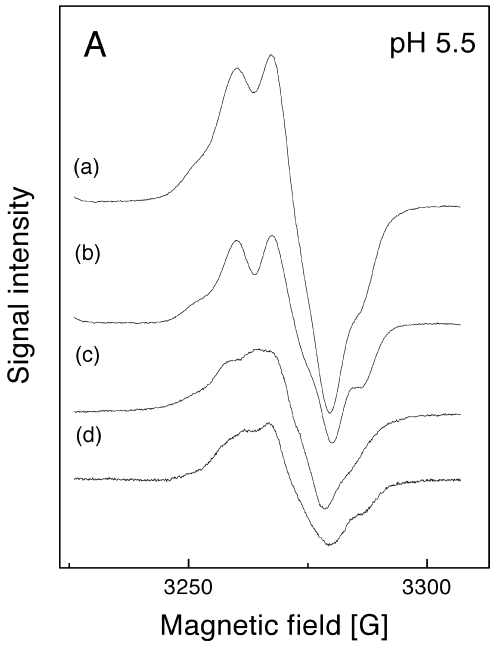

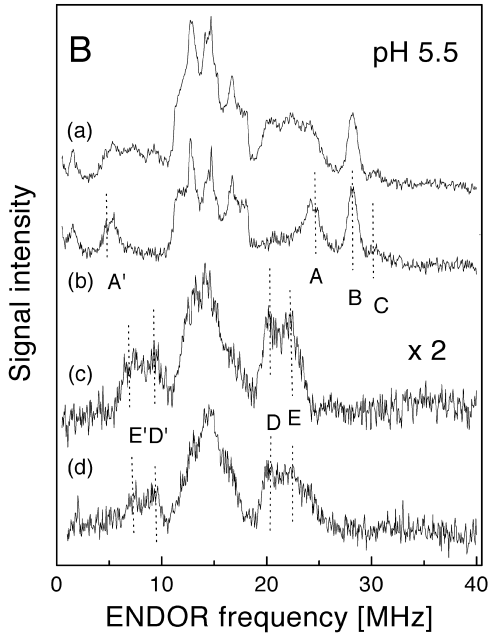

Fig. 2. CW-EPR (A) and pulsed ENDOR (B) spectra in Ca^{2+}-depleted PS II (a–c) and in Mn-depleted PS II membranes (d) at pH 5.5. Ca^{2+}-depleted membranes were frozen rapidly after illumination for 15 s at 253 K (a) and dark-adapted for 30 min at 0°C (b). Mn-depleted membranes were illuminated for 5 s at 253 K, then dark-adapted for 30 min at 0°C. Illumination minus dark-adaptation difference spectra (c, d). DCMU (50 μM) was added to sample suspension before illuminating Ca^{2+}-depleted membranes. CW-EPR and pulsed ENDOR conditions are described in the legend to Fig. 1.

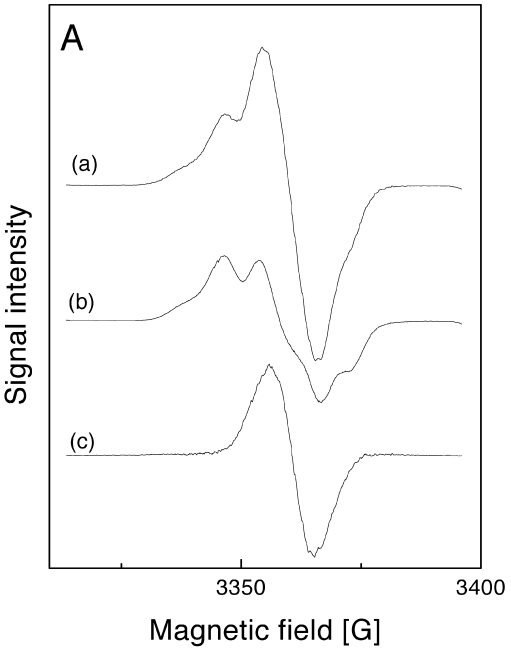

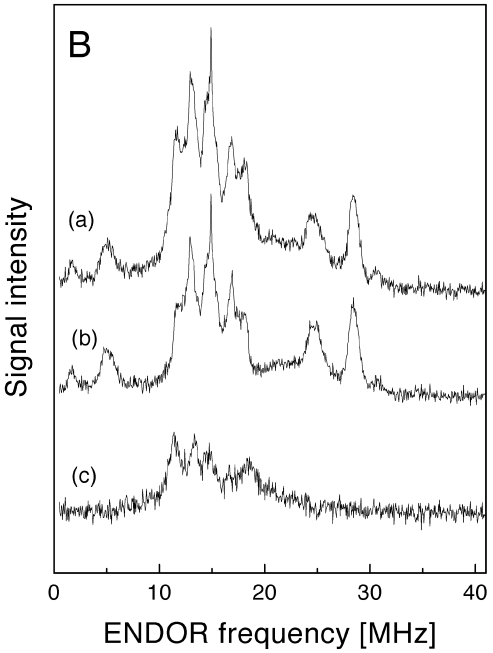

Fig. 3. CW-EPR (A) and pulsed ENDOR (B) spectra in Ca^{2+}-depleted PS II membranes at pH 5.5. The membranes were illuminated for 10 min at 77 K (a) and dark-adapted for 30 min at 0°C (b). Illumination minus dark-adaptation (a minus b) difference spectrum (c). Potassium ferricyanide (1 mM) was added to sample suspension before illuminating Ca^{2+}-depleted membranes. CW-EPR and pulsed ENDOR conditions are described in the legend to Fig. 1.

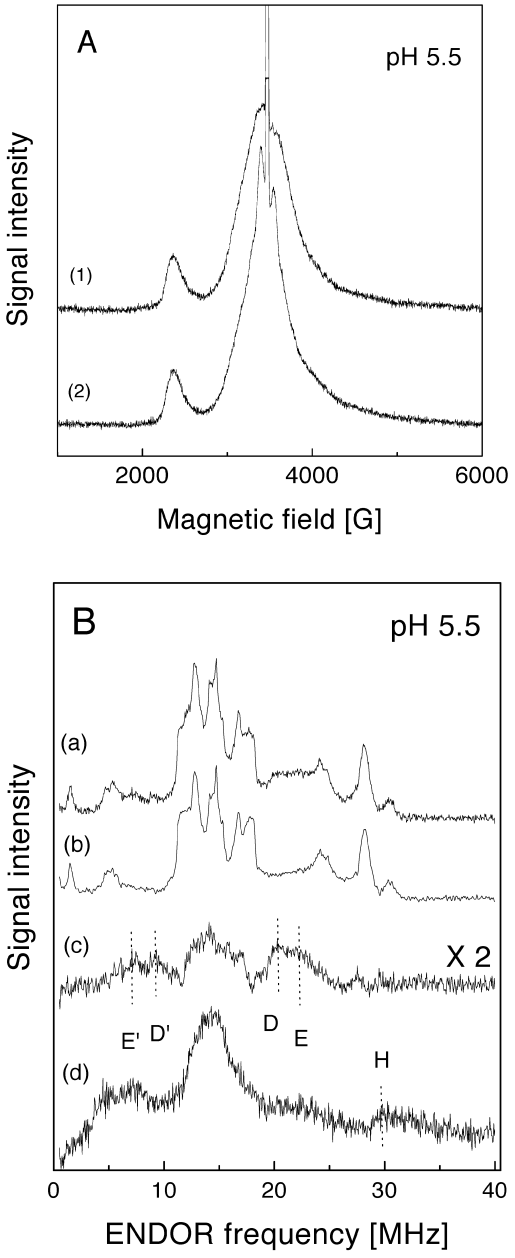

Fig. 4. Field-swept ESE (A) and pulsed ENDOR (B) spectra in Ca^{2+}-depleted PS II membranes at pH 5.5. Sample membranes were illuminated at 0°C for 1 min followed by dark-adaptation at 0°C for 30 min to form the dark-stable S_2-state. The preilluminated membranes (1) were frozen rapidly after illumination for 60 s at 0°C (2, d), or after illumination for 15 s at 253 K (a) followed by dark-adaptation for 30 min at 0°C (b). Illumination minus dark-adaptation (a minus b) difference spectrum (c). DCMU (50 μM) was added to sample suspension after preilluminating Ca^{2+}-depleted PS II membranes. ESE conditions; $\tau = 200$ ns; pulse repetition rate, 1 kHz. Pulsed ENDOR spectrum for doublet signal obtained at the 75 G upfield position from the center of the tyrosine radical. Doublet and $Y_Z^{\bullet}$ spectra were observed at 6 K and 30 K, respectively.
←

(trace c). As shown in Panel B, the ENDOR spectrum of Chl^+/Car^+ radicals (trace c) shows that there are several peaks around 10–20 MHz in the ENDOR frequency, but no D/D′ and E/E′ peaks found in the trapped $Y_Z^{\bullet}$ (see Fig. 2B). The results clearly indicate that the Chl^+/Car^+ radical does not contribute to the CW-EPR and ENDOR spectrum of the trapped $Y_Z^{\bullet}$ signal. The results are, furthermore, consistent with the report that 253 K illumination induced no Car^+ radical as well as very little Chl^+ radical [21–24].

Fig. 4A shows the field-swept ESE spectra at pH 5.5 in Ca^{2+}-depleted membranes, where sample membranes with OEC in the Ca^{2+}-depleted S_2 state (trace 1) were further illuminated at 0°C after adding DCMU (trace 2). Illumination induced a signal with a doublet splitting of about 150 G at $g \approx 2$ and a $Y_Z^{\bullet}$ signal concomitant with the decrease in intensity of the multiline signal by about 40%, consistent with the reported results [15]. The pulsed ENDOR spectrum in Fig. 4B of the $Y_Z^{\bullet}$ radical (trace c), trapped in the S_2 state was quite similar to that trapped by illuminating the membranes in the S_1 state (trace c in Fig. 2B) at pH 5.5, although the intensity was about half of that trapped in the S_1 state. The ENDOR spectrum of the doublet type signal (trace d) resembled that of the neutral $Y_Z^{\bullet}$ radical in Mn-depleted PS II membranes at pH 7.0 (trace d in Fig. 1B), confirming the involvement of the $Y_Z^{\bullet}$ radical in the doublet type signal [15,20]. The ENDOR spectrum of the trapped $Y_Z^{\bullet}$ radical differed considerably from that of the $Y_Z^{\bullet}$ radical responsible for the doublet-type signal (traces c and d in Fig. 4B).

4. Discussion

The present results demonstrated that the $Y_Z^{\bullet}$ radical trapped at pH 7.0 has considerably different CW-EPR and pulsed ENDOR spectra between Ca^{2+}-depleted and Mn-depleted PS II, but has quite similar CW and ENDOR spectra in both Ca^{2+}-depleted and Mn-depleted PS II membranes at pH 5.5. Consequently, the spectral features of the $Y_Z^{\bullet}$ radical trapped at pH 7.0 in Ca^{2+}-depleted PS II resembled

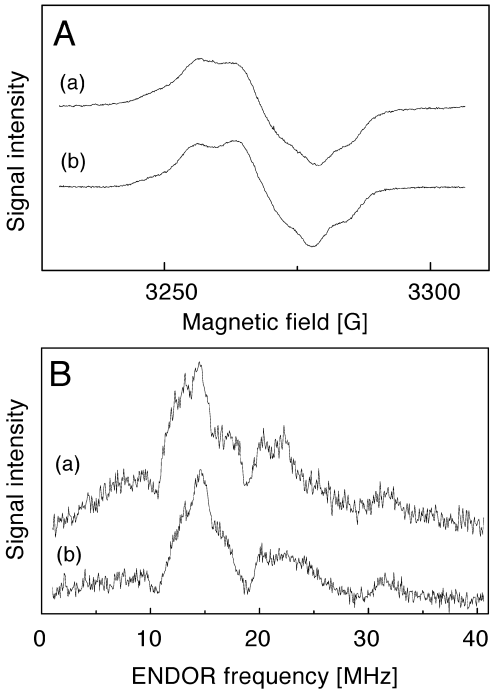

Fig. 5. CW-EPR and pulsed ENDOR spectra of $Y_Z^{\bullet}$ radical in Ca^{2+}-depleted PS II membranes at pH 7.0 (a), and spectra convoluted by $Y_Z^{\bullet}$ spectra in Mn-depleted PS II membranes at pH 5.5 and pH 7.0 (b). Spectra were taken from Figs. 1 and 2. The Mn-depleted CW-EPR spectra at pH 5.5 and pH 7.0 were summed in one-to-one ratio in terms of their integrated intensity, and the resulting spectrum was compared with the Ca^{2+}-depleted spectrum after normalization (panel A). The Mn-depleted pulsed ENDOR spectra at pH 5.5 and 7.0 were summed in one-to-one ratio in terms of integrated intensity of the matrix region (b), and the resulting spectrum was compared with the Ca^{2+}-depleted spectrum after normalization (a) (panel B).

those trapped in Mn-depleted PS II at pH 5.5. In Mn-depleted PS II, a decrease in the spin densities of the phenol-ring carbons $C_{(3),(5)}$ of tyrosine radical associated with a decrease in pH accounts for the EPR spectra changing from a neutral-pH (pH 7.0) to a low-pH form (pH 5.5) [10]. The similarity of the EPR and ENDOR spectra of the $Y_Z^{\bullet}$ radical at pH 7.0 in Ca^{2+}-depleted S_1 state to that in Mn-depleted PS II at pH 5.5 implies that the low-pH form of the $Y_Z^{\bullet}$ radical is already induced in Ca^{2+}-depleted PS II at pH 7.0 to some extent. It is of note in this context that optical absorption difference spectra of $Y_Z^{OX}-Y_Z$ at pH 7.5 in Ca^{2+}-depleted PS II is similar to that at pH 5.7 in Mn^{2+}-depleted PS II [25,26].

As shown in Fig. 5, the CW and ENDOR spectra of the trapped $Y_Z^{\bullet}$ radical at pH 7.0 in Ca^{2+}-depleted PS II in the S_1 state can be reasonably deconvoluted by the neutral-pH and the low-pH forms $Y_Z^{\bullet}$ radical spectra of Mn-depleted PS II. This may be because the pH dependence of the $Y_Z^{\bullet}$ radical spectrum in Ca^{2+}-depleted PS II is not identical to that in the Mn-depleted PS II; the conversion from the low-pH to the neutral-pH forms proceeds at a higher pH in Ca^{2+}-depleted than in Mn-depleted PS II. Alternatively, the $Y_Z^{\bullet}$ radical may be primarily produced as the low-pH form in Ca^{2+}-depleted PS II even at pH 7.0 and the $Y_Z^{\bullet}$ radical in Mn-depleted PS II centers partially generated during Ca^{2+}-depletion process may cause the neutral-pH form spectrum. Uncertainty as to the population of the PS II center damaged in the Ca^{2+}-depleted membranes and limited quantification of the EPR data preclude more detailed analysis. Therefore, which of these explanations is correct, cannot yet be determined.

The assumption that a neutral radical of tyrosine is responsible for the neutral-pH form $Y_Z^{\bullet}$ is rational since the spectrum of the neutral-pH form is quite similar to that of the $Y_D^{\bullet}$ radical that is assigned as being neutral radical [10,18–20]. The ENDOR spectrum of the low-pH form $Y_Z^{\bullet}$ radical has been accounted by the decreasing spin density on the ring carbon $C_{(3)}$ and $C_{(5)}$ to the value typical of the cation radical of tyrosine [10]. The direct formation of the cationic tyrosine radical is, however, unlikely without some abnormal microenvironment around the Y_Z tyrosine since the reported pK_a for deprotonation of the OH group in the oxidized phenols is generally the order of -2 [27]. Another interpretation is that Y_Z tyrosine is oxidized as a neutral radical but the spin densities on $C_{(3)}$ and $C_{(5)}$ are varied by something such as an electrostatic effect of positive charges localized in a close vicinity of Y_Z tyrosine. In either situation, an amino acid residue with a pK_a value at neutral pH are required to mediate the effect of ambient pH to the vicinity of Y_Z tyrosine. His 190, which is supposed to be pK_a value of 7, is proposed to locate close proximity to the Y_Z tyrosine [26,28,29]. His 190, therefore, is a good candidate for the putative residue to influence the pH dependence of the $Y_Z^{\bullet}$ radical formation.

In Ca^{2+}-depleted PS II, the Mn-cluster is oxidized at least up to the S_2 state. Therefore, the $Y_Z^{\bullet}$ radical in the low-pH form may be implicated in the electron transfer event between P680 and the Mn-cluster, at

least during the S_1 to S_2 transition. Whether or not the low-pH form $Y_Z^{\bullet}$ radical is functional in O_2-evolving PS II is of note, since the lumenal pH of the thylakoid is low under physiological illumination condition. In this context, the reported time-resolved CW-EPR spectrum of the $Y_Z^{\bullet}$ radical in O_2 evolving PS II [30] is similar to the low-pH form rather than the neutral-pH form spectrum, although the quality of the spectrum does not allow a decisive conclusion. Alternatively, the low-pH form $Y_Z^{\bullet}$ radical may be induced only in somehow distorted PS II centers regardless of the presence of the Mn-cluster in which the $Y_Z^{\bullet}$ radical is susceptible to the influence of external pH values, considering that the low-pH form is induced in Mn-depleted PS II and Ca^{2+}-depleted PS II that cannot evolve oxygen. Measurement of a high-quality spectrum of $Y_Z^{\bullet}$ radical in O_2 evolving PS II is required to clarify the functional aspect of the low-pH form $Y_Z^{\bullet}$ radical.

Upon illuminating Ca^{2+}-depleted PS II in the S_2 state under conditions that limit PS II to a single turnover, a doublet signal with a 150 G splitting line width appears around $g=2$ [15]. The pulsed ENDOR spectrum for the doublet signal induced at pH 5.5 was similar to that of the neutral radical of tyrosine (trace d in Fig. 3B). A slight difference in the hyperfine constant a_β of the β-methylene proton between the ENDOR spectra of the $Y_Z^{\bullet}$ radical at pH 7.0 (Fig. 1B, peak G) and the doublet signal can be explained by a small rotation of the dihedral angle θ between the plane formed by $C_{(1)}$, $C_{(\beta)}$ and $H_{(\beta)}$, and that determined by the p-orbital on $C_{(1)}$ and the $C_{(1)}$-$C_{(\beta)}$ bond (data not shown). The results therefore indicate that the neutral $Y_Z^{\bullet}$ radical participates in the doublet signal even at pH 5.5, in agreement with results obtained at pH 6.5 [15,20]. The generation of the neutral form $Y_Z^{\bullet}$ radical at pH 5.5, however, seems to contraindicate the finding that $Y_Z^{\bullet}$ radical trapped at this pH was the low-pH form as shown in Fig. 2B. The trapped $Y_Z^{\bullet}$ radical may be ascribed to the Mn-depleted PS II center contaminating the Ca^{2+}-depleted sample membranes. However, this possibility can be excluded because the low-pH form radical significantly contributed to the spectrum of the $Y_Z^{\bullet}$ radical trapped at pH 7.0 in the sample illuminated in the S_2-state (data not shown), at which the low-pH form $Y_Z^{\bullet}$ radical was not induced in Mn-depleted PS II as shown in Fig. 1. It has been proposed that an organic radical [15] or the Mn-cluster [20] contributes to the doublet signal as a magnetically coupled counterpart of the $Y_Z^{\bullet}$ radical. Therefore, such an interaction may influence the magnetic structure of the $Y_Z^{\bullet}$ radical to facilitate the neutral form, although how this is achieved remains to be resolved.

Acknowledgements

This work was supported by a Grant-in-Aid for Special Postdoctoral Researchers Program and Frontier Research Program at RIKEN given by STA, by grants (Nos. 09640783, 10129233) from MESC, and by the Hyogo Science and Technical Association Foundation.

References

[1] R.J. Debus, The manganese and calcium ions of photosynthesis oxygen evolution, Biochim. Biophys. Acta 1102 (1992) 269–352.
[2] V.K. Yachandra, K. Sauer, M.P. Klein, Manganese cluster in photosynthesis: where plants oxidize water to dioxygen, Chem. Rev. 96 (1996) 2927–2950.
[3] R.D. Britt, Oxygen evolution, in: D.R. Ort, C.F. Yocum (Eds.), Oxygen Photosynthesis: The Light Reaction, Kluwer Academic, 1996, pp. 137–164.
[4] T. Ono, T. Noguchi, Y. Inoue, M. Kusunoki, T. Matsushita, H. Oyanagi, X-ray detection of the period-four cycling of the manganese cluster in photosynthesis water oxidizing enzyme, Science 258 (1992) 1335–1337.
[5] T.A. Roelofs, W. Liang, M.J. Latimer, R.M. Cinco, A. Rompel, J.C. Andrews, K. Sauer, V.K. Yachandra, M.P. Klein, Oxidation states of the manganese cluster during the flash-induced S-state cycle of the photosynthetic oxygen-evolving complex, Proc. Natl. Acad. Sci. USA 93 (1996) 3335–3340.
[6] B.A. Barry, G.T. Babcock, Tyrosine radicals are involved in the photosynthetic oxygen-evolving system, Proc. Natl. Acad. Sci. USA 84 (1987) 7099–7103.
[7] B.A. Barry, M.K. El-Deeb, P.O. Sandusky, G.T. Babcock, Tyrosine radicals in photosystem II and related model compounds: Characterization by isotopic labeling and EPR spectroscopy, J. Biol. Chem. 265 (1990) 20139–20143.
[8] R.G. Evelo, A.J. Hoff, S.A. Dikanov, A.M. Tyryshkin, An ESEEM study of the oxidized electron donor of plant photosystem II: evidence that $D^{\bullet}$ is a neutral tyrosine radical, Chem. Phys. Lett. 161 (1989) 479–484.
[9] H.-J. Eckert, G. Renger, Temperature dependence of $P680^+$

reduction in O_2-evolving PS II membrane fragments at different redox states of the water oxidizing system, FEBS Lett. 236 (1988) 425–431.
[10] H. Mino, A.V. Astashkin, A. Kawamori, An EPR and Pulsed ENDOR Study of the Structure of Tyrosine $Z^{\bullet}$ in Mn-depleted Photosystem II, Spectrochim. Acta A 53 (1997) 1465–1483.
[11] Y. Kodera, H. Hara, A.V. Astashkin, A. Kawamori, T. Ono, EPR study of trapped tyrosine Z^{+} in Ca-depleted photosystem II, Biochim. Biophys. Acta 1232 (1995) 43–51.
[12] D.A. Berthold, G.T. Babcock, C.F. Yocum, A high resolved, oxygen-evolving photosystem II preparation from spinach thylakoid membranes, FEBS Lett. 134 (1981) 231–234.
[13] T. Ono, Y. Inoue, Effects of removal and reconstitution of the extrinsic 33, 24, and 16 kDa proteins on flash oxygen yield in photosystem II particles, Biochim. Biophys. Acta 850 (1986) 380–389.
[14] T. Ono, Y. Inoue, Removal of Ca by pH 3.0 treatment inhibits S_2 to S_3 transition in photosynthetic oxygen evolving photosystem II, Biochim. Biophys. Acta 973 (1989) 443–449.
[15] A.V. Astashkin, H. Mino, A. Kawamori, T. Ono, Pulsed EPR study of S_3' signal in the Ca^{2+}-depleted photosystem II, Chem. Phys. Lett. 272 (1997) 506–516.
[16] H. Mino, A. Kawamori, Microenvironments of tyrosine D^{+} and tyrosine Z^{+} in photosystem II studied by proton matrix ENDOR, Biochim. Biophys. Acta 1185 (1994) 213–220.
[17] E.R. Davies, A new pulsed ENDOR technique, Phys. Lett. 47A (1974) 1–2.
[18] C.J. Bender, M. Sahlin, G.T. Babcock, B.A. Barry, T.K. Chandrasheklar, S.P. Salowe, J. Stubbe, B. Lindstörm, L. Petersson, A. Ehrenberg, B.-M. Sjöberg, An ENDOR study of the tyrosyl free radical in ribonucleotide reductase from *Escherichia coli*, J. Am. Chem. Soc. 111 (1989) 8076–8083.
[19] S.E.J. Rigby, J.H.A. Nugent, P.J. O'Mally, The dark stable tyrosine radical of photosystem 2 studied in three species using ENDOR and EPR spectroscopies, Biochemistry 33 (1994) 1734–1742.
[20] M.L. Gilchrist Jr., J.A. Ball, D.W. Randall, R.D. Britt, Proximity of the manganese cluster of photosystem II to the redox-active tyrosine Y_Z, Proc. Natl. Acad. Sci. USA 92 (1995) 9545–9549.
[21] T. Noguchi, T. Mitsuka, Y. Inoue, Fourier transform infrared spectrum of the radical cation of β-carotene photoinduced in photosystem II, FEBS Lett. 356 (1994) 179–182.
[22] J. Hanley, Y. Deligiannakis, A. Pascal, P. Faller, A.W. Rutherford, Carotenoid oxidation in photosystem II, Biochemistry 38 (1999) 8189–8195.
[23] J.S. Vrettos, D.H. Stewart, J.C. de Paula, G.W. Brudvig, Low-temperature optical and resonance Raman spectra of a carotenoid cation radical in Photosystem II, J. Phys. Chem. B 103 (1999) 6403–6406.
[24] A. Miller, G.W. Brudvig, A guide to electron paramagnetic resonance spectroscopy of Photosystem II membranes, Biochim. Biophys. Acta 1056 (1991) 1–18.
[25] M. Haumann, W. Junge, Evidence for impaired hydrogen-bonding of tyrosine Y_Z in calcium-depleted photosystem II, Biochim. Biophys. Acta 1411 (1999) 121–133.
[26] M. Haumann, A. Mulkidjanian, W. Junge, Tyrosine-Z in Oxygen-evolving photosystem II: a hydrogen-bonded tyrosinate, Biochemistry 38 (1999) 1258–1267.
[27] W.T. Dixon, D. Murphy, Determination of the acidity constant of some phenol radical cation by means of electron spin resonance, Faraday II 72 (1976) 1221–1230.
[28] F. Mamedov, R.T. Sayre, S. Styring, Involvement of His 190 on the D1 protein in electron/proton transfer reactions on the donor side of photosystem II, Biochemistry 37 (1998) 14245–14256.
[29] A.A. Hays, I.R. Vassiliev, J.H. Golbeck, R.J. Debus, Roles of D1-His190 in the proton-coupled oxidation of tyrosine Y_Z in manganese-depleted photosystem II, Biochemistry 37 (1999) 11851–11865.
[30] C.W. Hoganson, G.T. Babcock, Electron-transfer events near the reaction center in O_2-evolving Photosystem preparations, Biochemistry 27 (1988) 5848–5855.